Arrest of WNT/β-catenin signaling enables the transition from pluripotent to differentiated germ cells in mouse ovaries

Morgane Le Rolle[a], Filippo Massa[a,b,1], Pam Siggers[c,1], Laurent Turchi[a,d,1], Agnès Loubat[a], Bon-Kyoung Koo[e,f], Hans Clevers[e], Andy Greenfield[c], Andreas Schedl[a], Marie-Christine Chaboissier[a,2], and Anne-Amandine Chassot[a,2,3]

[a]CNRS, Inserm, Institut de Biologie Valrose, Université Côte d'Azur, Parc Valrose, 06108 Nice Cedex 2, France; [b]Inovarion, 75005 Paris, France; [c]Mammalian Genetics Unit, Medical Research Council Harwell Institute, Oxfordshire OX11 0RD, United Kingdom; [d]Délégation à la Recherche Clinique et à l'Innovation, Centre Hospitalier Universitaire de Nice, 06000 Nice, France; [e]Hubrecht Institute, Royal Netherlands Academy of Arts and Sciences, 3584 CT Utrecht, The Netherlands; and [f]Institute of Molecular Biotechnology of the Austrian Academy of Sciences, Vienna Biocenter, 1030 Vienna, Austria

Edited by Janet Rossant, Gairdner Foundation, Toronto, Canada, and approved June 18, 2021 (received for review November 10, 2020)

Germ cells form the basis for sexual reproduction by producing gametes. In ovaries, primordial germ cells exit the cell cycle and the pluripotency-associated state, differentiate into oogonia, and initiate meiosis. Despite the importance of germ cell differentiation for sexual reproduction, signaling pathways regulating their fate remain largely unknown. Here, we show in mouse embryonic ovaries that germ cell–intrinsic β-catenin activity maintains pluripotency and that its repression is essential to allow differentiation and meiosis entry in a timely manner. Accordingly, in β-catenin loss-of-function and gain-of-function mouse models, the germ cells precociously enter meiosis or remain in the pluripotent state, respectively. We further show that interaction of β-catenin and the pluripotent-associated factor POU5F1 in the nucleus is associated with germ cell pluripotency. The exit of this complex from the nucleus correlates with germ cell differentiation, a process promoted by the up-regulation of *Znrf3*, a negative regulator of WNT/β-catenin signaling. Together, these data identify the molecular basis of the transition from primordial germ cells to oogonia and demonstrate that β-catenin is a central gatekeeper in ovarian differentiation and gametogenesis.

WNT/β-catenin | germ cells | POU5F1/OCT4 | differentiation | ovary

Primordial germ cells (PGCs) give rise to the next generation by differentiating from pluripotent progenitors into highly specialized, sexually dimorphic cells, the gametes, which in turn generate a totipotent zygote after fertilization. In mammals, PGCs colonize the embryonic gonad at midgestation (i.e., at 10.5 d post coitum [dpc] in mice). At this point, they become gonocytes but are still commonly termed PGCs until they stop proliferating in the gonad (1), gain their capacity for irreversible sexual differentiation, a process called germ cell licensing (2), and become either female (oogonia) or male (prospermatogonia) (3). In the mouse ovary, gonocytes express core pluripotency genes such as *Pou5f1* (also known as *Oct4*), *Nanog*, and *Sox2* (4, 5) until they move toward oogenesis. At 13.5 dpc, the germ cells stop proliferating in a cell-autonomous manner and enter meiosis following an intrinsic timing mechanism that is not fully understood (6, 7). This mechanism leads to epigenetic modifications (8, 9), including genome-wide loss of 5-methylcytosine and the activity of the methylcytosine dioxygenase TET1 and of the Polycomb Repressive Complex 1 (PRC1) to ensure the timely and efficient activation of germline reprogramming genes (9–12). In addition, expression of the transcriptional regulator *Zglp1*, induced by BMP2 signaling, confers the oogenic fate and stimulates meiosis entry (13, 14) by up-regulating the expression of *Stimulated by Retinoic Acid 8* (*Stra8*) and *Meiosin* (15, 16). So far, the intrinsic mechanisms that enable gonocytes to exit pluripotency, differentiate, and enter meiosis in a timely manner remain largely elusive. In PGCs, POU5F1 is essential for specification and survival (17, 18), but the lethality induced by *Pou5f1* genetic deletion prevented further analysis of its function at later stages of germ cell development. All-*trans* retinoic acid (ATRA) signaling has been long considered the key pathway that promotes *Stra8* expression and germ cell decision to enter meiosis (19, 20). However, recent reports show that ATRA signaling is dispensable for meiosis initiation and *Stra8* expression but rather increases the level of *Stra8* transcription (21, 22).

In the postnatal mouse testis, WNT/β-catenin signaling promotes spermatogonial stem cell proliferation and differentiation (23–25). Activation of WNT/β-catenin signaling is restricted by the expression of SHISA6, a cell-autonomous WNT-inhibitor, thus maintaining pluripotency in a subset of undifferentiated spermatogonia (25, 26). In mouse ovaries, WNT/β-catenin signaling is involved in the temporal control of somatic differentiation. Thus, impairing WNT/β-catenin activity by the genetic deletion of either *Ctnnb1* (encoding β-catenin) in *Sf1*-positive somatic cells, *Wnt4*, a ligand activating the WNT/β-catenin signaling, or *Rspo1*, an agonist of the same pathway, both produced by somatic cells (27), accelerates

Significance

In the mammalian ovary, primordial germ cells maintain a genomic program associated with pluripotency until they stop proliferating, move toward oogenesis, and enter meiosis. The molecular mechanisms that enable primordial germ cells to exit pluripotency and enter meiosis in a timely manner are unclear, and their identification represents a major challenge in reproductive biology because the fertility of each individual depends on this. Evidence that cessation of germ cell proliferation is a cell-autonomous event, unrelated to the number of cell divisions, led to a search for an intrinsic timing mechanism that has long remained elusive. We describe here that WNT/β-catenin signaling regulates this timing and coordinates the transition from pluripotent to gametogenesis-competent germ cells.

Author contributions: A.-A.C. designed research; M.L.R., F.M., P.S., A.L., and A.-A.C. performed research; B.-K.K., H.C., A.G., and A.S. contributed new reagents/analytic tools; M.L.R., L.T., and A.-A.C. analyzed data; and M.-C.C. and A.-A.C. wrote the paper.

The authors declare no competing interest.

This article is a PNAS Direct Submission.

[1]F.M., P.S., and L.T. contributed equally to this work.

[2]M.-C.C. and A.-A.C. contributed equally to this work.

[3]To whom correspondence may be addressed. Email: Amandine.CHASSOT@univ-cotedazur.fr.

This article contains supporting information online at https://www.pnas.org/lookup/suppl/doi:10.1073/pnas.2023376118/-/DCSupplemental.

Published July 23, 2021.

the differentiation of the fetal granulosa cells into mature granulosa cells (28) and eventually triggers transdifferentiation into somatic testicular (Sertoli) cells (27, 29, 30). In addition, WNT/β-catenin signaling is active in gonocytes, and the genetic deletion of *Rspo1* or *Wnt4* also impairs germ cell sexual differentiation (31, 32). Nevertheless, it was not possible so far to address whether the effect on gonocytes of *Rspo1* or *Wnt4* genetic deletion was direct or indirect. Indeed, the abnormal sexual differentiation of the somatic cells in the XX *Rspo1*$^{-/-}$ or *Wnt4*$^{-/-}$ gonads (27, 29) likely impacts germ cell development and prevents determination of the specific function of WNT/β-catenin signaling in female germ cells.

The interaction of secreted WNTs with Frizzled and LRP5/6 receptors activates the β-catenin-dependent (canonical) pathway (33). In the resting state, cytosolic and nuclear pools of β-catenin must be maintained at a very low level through rapid turnover of free β-catenin by the degradation complex composed by APC, AXIN2, CK1, and GSK3β (34). GSK3β mediates β-catenin phosphorylation, eventually leading to its degradation by the 26S proteasome (35, 36). Upon WNT activation, the degradation complex is anchored at the membrane, and cytoplasmic β-catenin is not degraded and enters the nucleus, where it associates with transcription factors, notably TCF and LEF1, to regulate the transcription of target genes. The availability of the WNT-receptor complex at the membrane, critical for the regulation of WNT signaling, depends on ZNRF3 and RNF43. Indeed, these related transmembrane E3 ubiquitin ligases balance adequate levels of WNT activity by selectively ubiquitinating Frizzled receptors, thereby targeting them for degradation (37, 38).

We have now addressed the specific role of WNT/β-catenin signaling in female gonocytes by genetic deletion of *Ctnnb1* in vivo. The genetic deletion of *Ctnnb1* in the somatic progenitor cells inhibits *Bmp2* expression, promoting the maintenance of the pluripotency in the gonocytes and impairing meiosis entry. By contrast, genetic deletion of C*tnnb1* in gonocytes is accompanied by changes in chromatin accessibility including POU5F1-regulated loci. The gonocytes precociously exit pluripotency, differentiate, and eventually enter meiosis. Finally, maintenance of WNT receptor activity by the genetic deletion of *Znrf3* maintains gonocyte pluripotency, revealing that ZNRF3 negatively regulates WNT/β-catenin signaling in gonocytes to allow them to differentiate. Together, our results demonstrate that a finely tuned timing in WNT/β-catenin signaling activity controls the differentiation of the gonocytes and their entry into meiosis.

Results

β-Catenin Activity in Somatic Cells Promotes Meiosis Entry through Regulation of *Bmp2*. To differentiate between *Ctnnb1* functions in different ovarian cell types, we generated two genetic models allowing a cell-specific deletion of *Ctnnb1* using either the *Wt1-CreERT2* recombinase that is active in the somatic cells of the ovary (Fig. 1 and *SI Appendix*, Fig. S1) (39) or the *Sox2-CreERT2* recombinase (40) that is expressed in the primordial germ cells (Fig. 2) (40). In both models (*Wt1-CreERT2;Ctnnb1*$^{flox/flox}$ and *Sox2-CreERT2;Ctnnb1*$^{flox/flox}$ embryos), conditional deletion of *Ctnnb1* was induced upon two tamoxifen (TAM) treatments at 9.5 and 10.5 dpc (Fig. 2*B* and *SI Appendix*, Fig. S1*B*). We first focused our attention on the effects of *Ctnnb1* genetic deletion in somatic cells (*Wt1-CreERT2;Ctnnb1*$^{flox/flox}$ animals). In this condition, both β-catenin and LEF1 nuclear staining were absent from somatic cells in *Wt1-CreERT2;Ctnnb1*$^{flox/flox}$ animals (*SI Appendix*, Fig. S1*C*). In contrast, their expression remained in germ cells (*SI Appendix*, Fig. S1*C*). This demonstrates that WNT/β-catenin signaling was efficiently inactivated in a cell-specific fashion in this model.

At 13.5 dpc, the expression of FOXL2, which marks pregranulosa cells (41, 42), was not affected in *Wt1-CreERT2;Ctnnb1*$^{flox/flox}$ gonads compared to control gonads, and the Sertoli cell markers SOX9 and AMH were not expressed (*SI Appendix*, Fig. S1), indicating that the sexual identity of the FOXL2-positive somatic cells was not compromised at this stage of development. Moreover, we found that the proliferation of both germ cell and somatic cell populations was not significantly affected by the somatic *Ctnnb1* loss-of-function (*SI Appendix*, Fig. S2*B*). We next checked that deleting *Ctnnb1* from the somatic progenitor cells recapitulated the phenotypes of the *Rspo1* and the *Wnt4* genetic deletions (27, 28, 31, 32) (i.e., maintenance of POU5F1 and SSEA1 expression in germ cells) (Fig. 1*A* and *SI Appendix*, Fig. S2*A*), ectopic expression of the male germ cell marker *Nanos2* (Fig. 1*B*), and decrease of *Stra8* expression (Fig. 1*B*). *Stra8* mRNA was severely decreased in germ cells from *Wt1-CreERT2;Ctnnb1*$^{flox/flox}$ animals. Strikingly, we found almost no expression of *Bmp2* mRNA, encoding a secreted factor required for the oogenic fate and meiosis entry of PGC-like cells in culture (13, 43), in 13.5 dpc *Wt1-CreERT2;Ctnnb1*$^{flox/flox}$ gonads compared to the control gonads. This suggests that *Bmp2* expression is regulated by the WNT/β-catenin activity in somatic cells and promotes the molecular crosstalk between somatic cells and gonocytes and, indirectly, germ cell entry into meiosis (Fig. 1*B*).

β-Catenin Activity Controls Cell Cycle Exit in Germ Cells. We next focused our attention on the consequences of *Ctnnb1* genetic deletion in primordial germ cells (*Sox2-CreERT2;Ctnnb1*$^{flox/flox}$ animals). In this condition, both β-catenin and LEF1 nuclear staining were absent from germ cell nuclei in *Sox2-CreERT2;Ctnnb1*$^{flox/flox}$ animals (Fig. 2*D* and *SI Appendix*, Fig. S3), whereas their expression remained in somatic cells. To quantify *Axin2* expression in germ cells, we used mice harboring both the CRE-recombinase reporter (named *mTmG* reporter hereafter) (44) and the *Sox2-CreERT2* recombinase. In this model, the expression of the membrane-tagged GFP was specifically activated in the majority of the germ cells after tamoxifen (TAM) administration, allowing fluorescent-activated cell sorting (FACS) purification. At 12.5 dpc, *Axin2* mRNA levels were strongly reduced in gonocytes (Fig. 2*E*), indicating an efficient inactivation of WNT/β-catenin signaling. It is noteworthy that *Ctnnb1* deletion in gonocytes did not affect the development of the embryos (Fig. 2*C*) nor the somatic cell proliferation (Fig. 2*C*) or sexual differentiation of the ovaries, as evidenced by the expression of FOXL2 and the absence of SOX9 and AMH expression (Fig. 2*D* and *SI Appendix*, Fig. S3).

To assess the contribution of WNT/β-catenin signaling in germ cell proliferation, we performed immunostaining using MKI67 antibody, which marks all stages of cell-cycle progression. Whereas germ cell proliferation was not modified at 11.5 dpc, quantification of the number of MKI67-positive versus total germ cells (TRA98-positive) at 12.5 and 13.5 dpc highlighted a significant decrease of proliferative germ cells in the TAM-treated *Sox2-CreERT2;Ctnnb*$^{flox/flox}$ ovaries compared to controls, with 27.72 to 17.16% fewer proliferative germ cells, respectively ($P = 0.000939$). Somatic cell proliferation, by contrast, was not impacted (Figs. 2*C* and 3*A* and *SI Appendix*, Fig. S4). As a consequence, the total number of germ cells was decreased in the *Sox2-CreERT2;Ctnnb*$^{flox/flox}$ ovaries compared to controls at 12.5 dpc (Fig. 3*A*). This suggests that germ cells stopped proliferating in the *Sox2-CreERT2;Ctnnb1*$^{flox/flox}$ ovaries and exited the cycling state earlier than in control ovaries. These results indicate that β-catenin signaling instructs the mitotic cell-cycle of gonocytes.

β-Catenin Regulates the Timing of Germ Cell Differentiation. We next examined the differentiation of germ cells in the absence of WNT/β-catenin signaling activity in *Sox2-CreERT2;Ctnnb1*$^{flox/flox}$ embryonic ovaries. We found that the mRNA levels of the pluripotency-associated markers *Pou5f1 (Oct4)*, *Sox2*, and *Nanog* were significantly reduced in purified germ cells from 12.5 dpc gonads (Fig. 2*E*). This was accompanied by an increase in mRNA expression levels of *Piwil2* and *Ddx4*, two markers of germ cell differentiation, suggesting that gonocytes precociously differentiated when canonical WNT/β-catenin signaling was down-regulated. POU5F1-positive gonocytes were less abundant in the mutant ovaries at 12.5 dpc, with some DDX4-positive gonocytes being devoid of

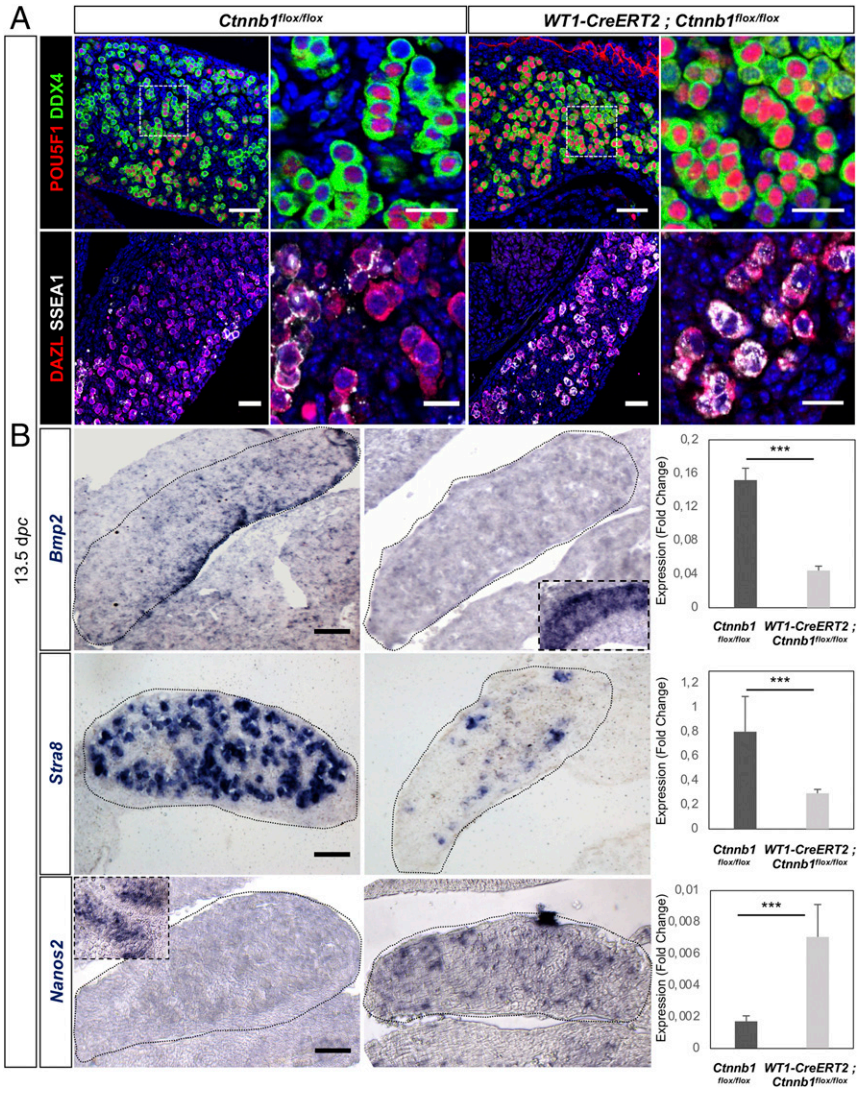

Fig. 1. *Ctnnb1* deletion in the somatic progenitor cells indirectly impairs germ cell licensing. (*A*, *Upper*) Immunodetection of POU5F1 (red) and DDX4 (germ cells, green) in 13.5 dpc control (*Ctnnb1*$^{flox/flox}$) and *Wt1-CreERT2; Ctnnb1*$^{flox/flox}$ ovaries. (*Lower*) Immunodetection of DAZL (red) and SSEA1 (white) in 13.5 dpc control (*Ctnnb1*$^{flox/flox}$) and *Wt1-CreERT2; Ctnnb1*$^{flox/flox}$ ovaries. DAPI (blue): nuclei. (Scale bars: 50 or 20 μm.) (*B*) In situ hybridization using *Bmp2*, *Stra8*, and *Nanos2* riboprobes at 13.5 dpc in control (*Ctnnb1*$^{flox/flox}$, *Left*) and *Wt1-CreERT2; Ctnnb1*$^{flox/flox}$ (mutant, *Right*) ovaries (dotted circles). (Scale bars: 50 μm.) (*Inset*) *Bmp2* expression in the developing bone of !the same *Wt1-CreERT2; Ctnnb1*$^{flox/flox}$ mutant animal as positive control. (*Inset*) *Nanos2* expression in sex cords from 13.5 dpc testis as positive control. Histograms: qRT-PCR analysis of *Bmp2*, *Stra8*, and *Nanos2 (*expression in 13.5 dpc control (*Ctnnb1*$^{flox/flox,}$ gray) and *Wt1-CreERT2; Ctnnb1*$^{flox/flox}$ (pale gray) ovaries. Student's *t* test, unpaired. Bars represent mean + SEM, $n = 6$ individual gonads. ***$P < 0.001$.

POU5F1, whereas gonocytes were positive for both markers in control ovaries (Fig. 2*B* and *SI Appendix*, Fig. S4). We next analyzed the expression of SSEA1 and POU5F1, two pluripotency-associated markers, and DAZL and DDX4, two markers of germ cell differentiation, at 13.5 dpc. We found that the number of SSEA1- or POU5F1-positive germ cells was significantly reduced from 45 to 25% and from 40 to 15% of total germ cells, respectively, whereas the number of DAZL- or DDX4-positive germ cells was significantly increased from 55 to 75% and from 60 to 85%, respectively, in mutant compared to control ovaries (Fig. 3*B*). We next verified that functional heterozygosity of the *Sox2* allele due to the insertion of the *Sox2-CreERT2* transgene did not impair the fate of the germ cells. Immunodetection of POU5F1 and SOX2 highlighted that these two proteins were similarly expressed in oil-treated *Sox2-CreERT2;Ctnnb*$^{flox/flox}$ compared to *Ctnnb1*$^{flox/flox}$ embryonic ovaries, while POU5F1 expression was severely impaired and SOX2 expression was absent in TAM-treated *Sox2-CreERT2;Ctnnb*$^{flox/flox}$ ovaries (*SI Appendix*, Fig. S5). Our data demonstrate that the absence of WNT/β-catenin activity impaired gonocyte pluripotency and triggered a precocious differentiation, suggesting that β-catenin is required to maintain the pluripotency state in gonocytes.

Chromatin Accessibility is Modified in Germ Cells in Absence of WNT/β-Catenin Signaling. Chromatin state is critical for the timing of germ cell differentiation in mouse ovaries (9, 11). To investigate whether WNT/β-catenin signaling triggers chromatin modifications in gonocytes, we performed an assay for transposase-accessible chromatin (ATAC-seq) to map open and closed chromatin. We surveyed differences in chromatin accessibility between control and *Sox2-CreERT2;Ctnnb1*$^{flox/flox}$ germ cells isolated from 12.5 dpc embryos, when gonocytes initiate the transition from pluripotency to differentiation (Fig. 4 and *SI Appendix*, Fig. S6). The vast majority of the regions displaying significant differences in chromatin accessibility were localized both in promoters and intergenic regions and appeared less accessible upon the loss of *Ctnnb1* (46 out of 48 regions) (*SI Appendix*, Fig. S6 *A* and *B*). Gene Ontology analysis revealed that these genomic regions were associated with differentiation and transcriptional regulation, chromatin modification, chromosome X reactivation, meiosis, and WNT/β-catenin signaling (Fig. 4*A*), which are all features of gonocyte development. Notably, the genomic regulatory regions that were more closed in the absence of *Ctnnb1* included *Ncoa1* and *Tbl1x*, which enhance the transcriptional activity through chromatin remodelling by mediating exchanges of corepressors for coactivators (45, 46), *Tdrd12*, which is involved in Piwi-interacting RNA biogenesis (47) and *Tsix*/*Xist*, required for chromosome X dosage compensation (48) (*SI Appendix*, Fig. S6*C*). Moreover, mutations in some of these genes, such as *Ncoa1* and *Tdrd12*, cause spermatogenesis defects (47, 49). Together, these results indicate that WNT/β-catenin

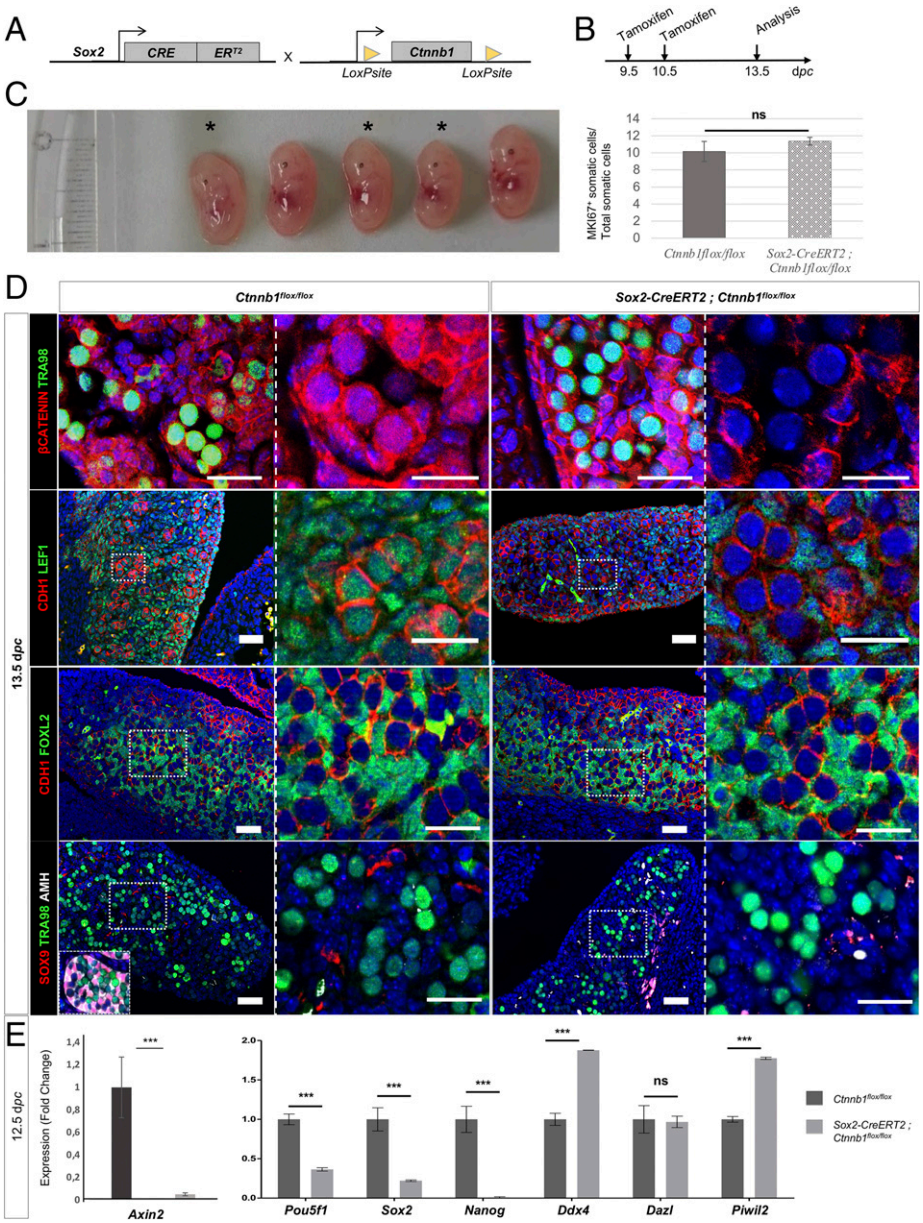

Fig. 2. *Ctnnb1* deletion in the primordial germ cells does not affect the size of the animals nor the somatic cell differentiation but impairs germ cell differentiation. (*A*) Schematic representation of the strategy used to delete Lox-P–flanked *Ctnnb1* (encoding β-catenin) in the primordial germ cells in an inducible manner using the *Sox2-CreERT2* line specifically expressed in germ cells. (*B*) Protocol of induction of *Sox2-CreERT2* (9.5 and 10.5 dpc onward). TAM: Tamoxifen. (*C*) Macroscopic view of a 13.5 dpc litter containing control (*Ctnnb1*$^{flox/flox}$) and *Sox2-CreERT2; Ctnnb1*$^{flox/flox}$ (black asterisks) embryos displaying any major physical abnormalities and normal size. Histograms: quantification of the percentage of both MKI67-positive somatic cells (i.e., proliferating somatic cells) in 12.5 dpc control (*Ctnnb1*$^{flox/flox}$) and *Sox2-CreERT2; Ctnnb1*$^{flox/flox}$ ovaries. Student's *t* test, unpaired. Bars represent mean + SEM, ns: not significant. (*D*) Immunodetection of β-catenin (red) and TRA98 (germ cells, green) (*Upper*) and CDH1 (red) and LEF1 (green) (*Lower*) in 13.5 dpc control (*Ctnnb1*$^{flox/flox}$) and *Sox2-CreERT2; Ctnnb1*$^{flox/flox}$ ovaries. DAPI (blue): nuclei. (Scale bars: 50 or 20 μm.) Immunodetection of CDH1 (germ cells, red) and FOXL2 (pregranulosa cells, green) (*Upper*) and SOX9 (male somatic cells, red), AMH (male somatic cells, white), and TRA98 (germ cells, green) (*Lower*) in 13.5 dpc control (*Ctnnb1*$^{flox/flox}$) and *Sox2-CreERT2; Ctnnb1*$^{flox/flox}$ ovaries. (*Inset*) The 13.5 dpc XY embryonic gonad used as a positive control for SOX9 and AMH expression. DAPI (blue): nuclei. (Scale bars: 50 or 20 μm.) (*E*, *Left*) qRT-PCR analysis of *Axin2* expression in purified germ cells from 12.5 dpc control (*Ctnnb1*$^{flox/flox}$) (dark gray) and *Sox2-CreERT2; Ctnnb1*$^{flox/flox}$ (pale gray) ovaries. Student's *t* test, unpaired. Bars represent mean + SEM, $n = \sim$30,000 germ cells FACS-purified from 20 individual gonads. ***$P < 0.001$. (*Right*) qRT-PCR analysis of *Pou5f1*, *Sox2*, *Nanog*, *Ddx4*, and *Piwil2* expression in purified germ cells from 12.5 dpc control (*Ctnnb1*$^{flox/flox}$) (dark gray) and *Sox2-CreERT2; Ctnnb1*$^{flox/flox}$ (pale gray) ovaries. Student's *t* test, unpaired. Bars represent mean + SEM, n = ~30,000 germ cells FACS-purified from 20 individual gonads. ***$P < 0.001$.

activity regulates the program of germ cell differentiation including modifications of chromatin accessibility.

POU5F1 and β-Catenin Physically Interact and Exit Nucleus during Germ Cell Differentiation. Remarkably, among the genomic sites with reduced accessibility in the absence of *Ctnnb1* that were revealed by the ATAC-seq assay, 20.69% of them exhibited binding motifs for the transcription factor POU5F1 ($P = 0.000001$) (Fig. 4*B*), suggesting that POU5F1 and β-catenin cooperate to regulate target loci involved in germ cell differentiation. These observations prompted us to further analyze POU5F1 expression and activity during germ cell differentiation. Whereas POU5F1

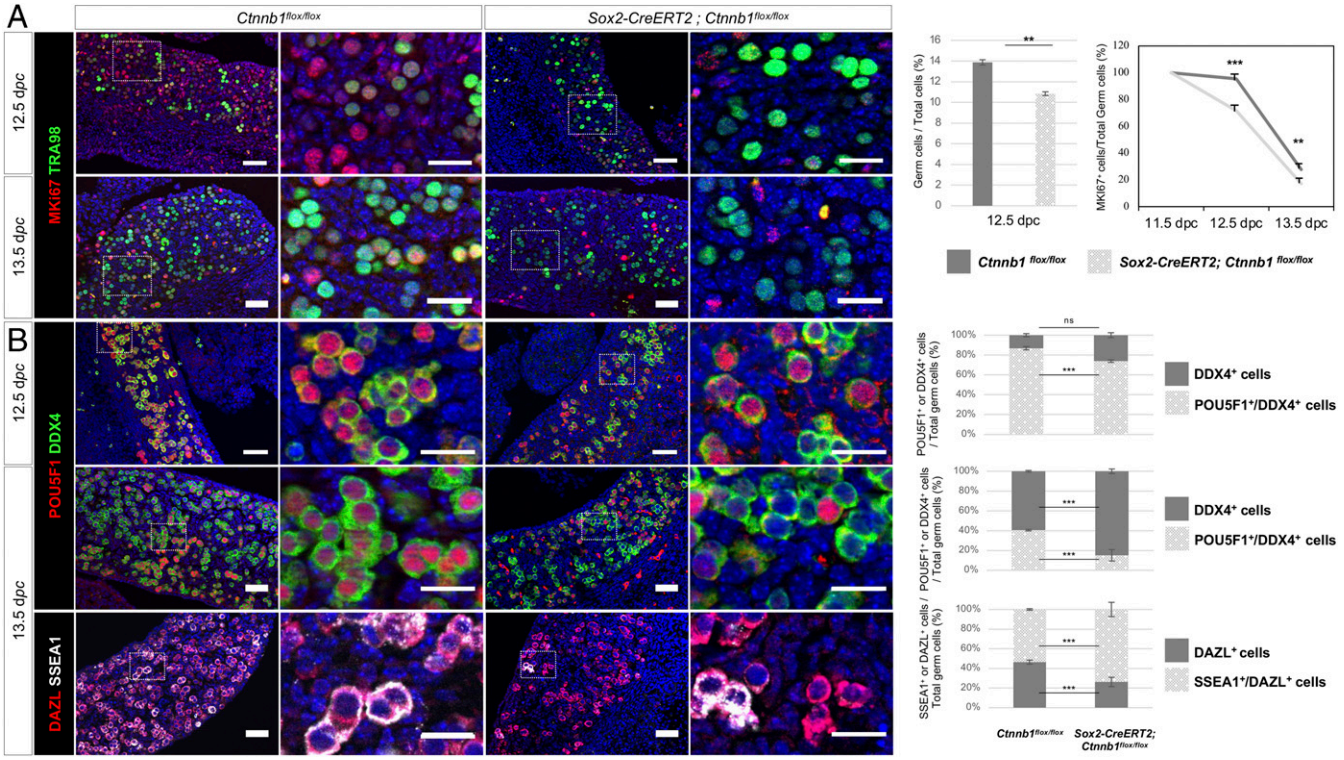

Fig. 3. Germinal ablation of *Ctnnb1* impairs gonocyte proliferation and differentiation. (*A*, *Left*) Immunodetection of MKI67 (proliferating cells, red) and TRA98 (germ cells, green) in 12.5 and 13.5 dpc control (*Ctnnb1*$^{flox/flox}$) and *Sox2-CreERT2; Ctnnb1*$^{flox/flox}$ ovaries. DAPI (blue): nuclei. (Scale bars: 50 or 20 μm.) Histograms: quantification of the percentage of total germ cells (TRA98-positive cells) versus total gonadal cells in 12.5 dpc control (*Ctnnb1*$^{flox/flox}$, dark gray) and *Sox2-CreERT2; Ctnnb1*$^{flox/flox}$ (dotted gray) ovaries. Graphs (*Right*): quantification of both MKI67- and TRA98-positive cells (i.e., proliferating germ cells) in 11.5, 12.5, and 13.5 dpc control (*Ctnnb1*$^{flox/flox}$, dark gray) and *Sox2-CreERT2; Ctnnb1*$^{flox/flox}$ (dotted pale gray) ovaries. Student's *t* test, unpaired. Bars represent mean + SEM; $^{**}P < 0.01$ and $^{***}P < 0.001$. (*B*, *Upper*) Immunodetection of POU5F1 (red) and DDX4 (germ cells, green) in 12.5 and 13.5 dpc control (*Ctnnb1*$^{flox/flox}$) and *Sox2-CreERT2; Ctnnb1*$^{flox/flox}$ ovaries. (*Lower*) Immunodetection of DAZL (red) and SSEA1 (white) in 13.5 dpc control (*Ctnnb1*$^{flox/flox}$) and *Sox2-CreERT2; Ctnnb1*$^{flox/flox}$ ovaries. DAPI (blue): nuclei. (Scale bars: 50 or 20 μm.) (*Right*) Histograms: quantification of DDX4-positive cells (dark gray) and POU5F1-DDX4 double positive cells (dotted gray) (%) in control (*Ctnnb1*$^{flox/flox}$) and *Sox2-CreERT2; Ctnnb1*$^{flox/flox}$ ovaries from 12.5 (*Upper*) and 13.5 dpc (*Middle*) embryos after immunodetection. Quantification of DAZL-positive cells (dark gray) and SSEA1-DAZL double positive cells (dotted gray) (%) (*Lower*) in control (*Ctnnb1*$^{flox/flox}$) and *Sox2-CreERT2; Ctnnb1*$^{flox/flox}$ ovaries from 13.5 dpc embryos after immunodetection. Student's *t* test, unpaired. Bars represent mean + SEM. ns: not significant; $^{***}P < 0.001$.

was detected in the nucleus of control germ cells, POU5F1 was readily detectable in the cytoplasm of ~32% of germ cells ($P = 0.011$) in *Sox2-CreERT2;Ctnnb1*$^{flox/flox}$ ovaries at 12.5 dpc (Fig. 4 *C* and *D*). This increased to 82% of the germ cells at 13.5 dpc, whereas only 31% of control germ cells harbored cytoplasmic POU5F1 ($P = 0.000027$) (Fig. 4 *C* and *E*). We next investigated whether premature localization of POU5F1 to the cytoplasm in the absence of β-catenin modified the expression of POU5F1 target genes. We quantified mRNA levels of *Pou5f1* and *Dppa3*, which are targets of POU5F1 in embryonic stem cells (ESCs) (50, 51) and are expressed in pluripotent mouse germ cells (52). *Pou5f1* and *Dppa3* levels were significantly down-regulated in the *Sox2-CreERT2;Ctnnb*$^{flox/flox}$ germ cells at 13.5 dpc (Fig. 4*F*), suggesting that POU5F1 transcriptional activity was decreased in *Sox2-CreERT2;Ctnnb1*$^{flox/flox}$ germ cells.

To gain further insight into the mechanism of β-catenin action, we investigated the localization of POU5F1 and β-catenin by confocal microscopy during germ cell differentiation in wild-type ovaries in vivo. Whereas both of them were detected in the nucleus of gonocytes at 12.5 dpc, they were mostly localized to the cytoplasm at 14.5 dpc (Fig. 5 *A* and *B*). These observations further suggest that POU5F1 and β-catenin colocalize to the nucleus or the cytoplasm depending on the level of WNT/β-catenin activity. To investigate whether POU5F1 and β-catenin physically interact, we performed immunoprecipitation experiments on protein extracts from 12.5 and 14.5 dpc ovaries, using a POU5F1-specific antibody (Fig. 5*C*). At 12.5 dpc, POU5F1 was weakly associated with β-catenin. In contrast, at 14.5 dpc, POU5F1 strongly coimmunoprecipitated with β-catenin and with CDH1, which is expressed outside of the nucleus (Fig. 5*C*). To verify POU5F1 and β-catenin interaction in the germ cell cytoplasm at 14.5 dpc, we performed cell fractionation experiments followed by immunoprecipitation using a POU5F1-specific antibody and checked the expression of POU5F1 and β-catenin in either nuclear or cytoplasmic/membranous fractions by Western blot (Fig. 5*D*). We first validated the purity of each fraction by analyzing the expression of different markers such as CDH1 and GAPDH for the cytoplasmic fraction and RNA Polymerase II and Histone H3 for the nuclear fraction (Fig. 5*D*). Even though POU5F1 and β-catenin were still weakly detected in the nuclear fraction, they were mainly expressed in the cytoplasmic fraction where they coimmunoprecipitated, further confirming the cytoplasmic localization and association of the two proteins at this stage. Taken together, these observations indicate that β-catenin and POU5F1 physically interact in germ cells, an association which may maintain the localization of both in the nucleus of pluripotent germ cells in vivo until they enter differentiation.

β-Catenin Activity Regulates the Timing of Meiosis Initiation. To investigate whether germ cells entered meiosis in the *Sox2-CreERT2;Ctnnb1*$^{flox/flox}$ ovaries, we examined the profile of *Stra8* expression by in situ hybridization analyses and qRT-PCR at 12.5 and 13.5 dpc

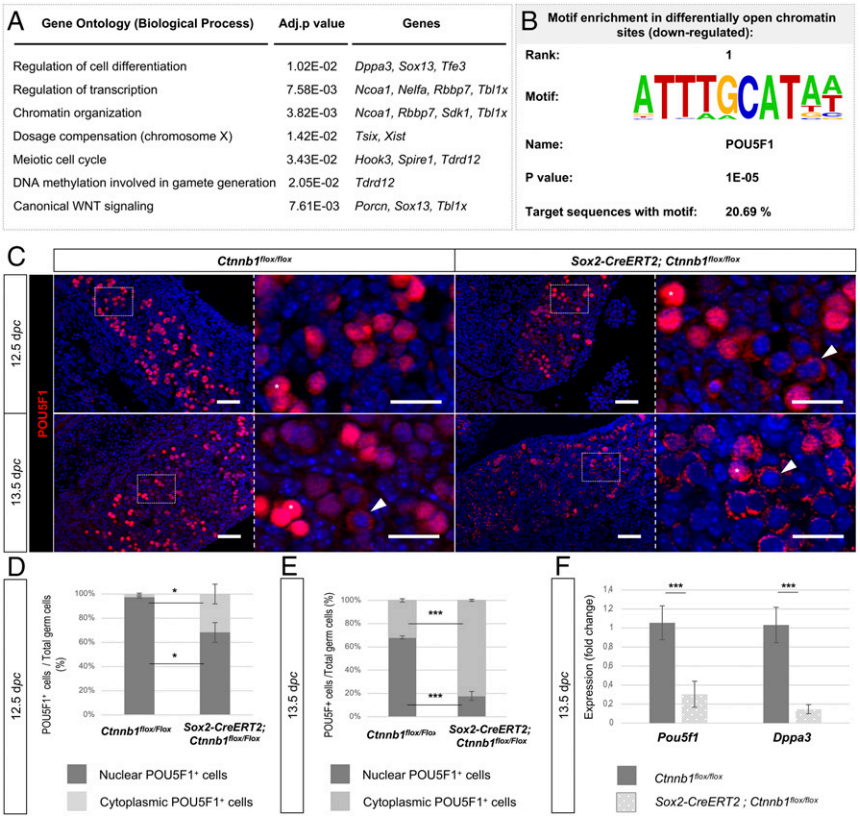

Fig. 4. Germinal ablation of *Ctnnb1* triggers POU5F1 precocious exit from germ cell nucleus. (*A*) Gene Ontology terms associated with chromatin regions that are differentially opened/closed between control (*Ctnnb1*$^{flox/flox}$) and *Sox2-CreERT2; Ctnnb1*$^{flox/flox}$ isolated germ cells from 12.5 dpc ovaries based on PANTHER classification software (log fold change ≥ 0.5) and names of the corresponding genes. Adjusted *P* values are indicated. *n* = 50,000 germ cells in duplicate for each genotype. (*B*) Motif enrichment analysis of differentially open chromatin regions (with adjusted *P* value and percentage of target sequences with motif). POU5F1 fixation motif was found at first rank among genomic regions being down-regulated between control (*Ctnnb1*$^{flox/flox}$) and *Sox2-CreERT2; Ctnnb1*$^{flox/flox}$ isolated germ cells. (*C*) Immunodetection of POU5F1 (red) in 12.5 and 13.5 dpc control (*Ctnnb1*$^{flox/flox}$) and *Sox2-CreERT2; Ctnnb1*$^{flox/flox}$ ovaries. DAPI (blue): nuclei. (Scale bars: 50 or 20 μm.) (*D* and *E*) Histograms: quantification of the percentage of nuclear (gray) and cytoplasmic (dotted gray) POU5F1-positive cells in 12.5 and 13.5 dpc control (*Ctnnb1*$^{flox/flox}$, gray) and *Sox2-CreERT2; Ctnnb1*$^{flox/flox}$ (dotted gray) ovaries. Student's *t* test, unpaired. Bars represent mean + SEM. **P* < 0.05 and ****P* < 0.001. (*F*) qRT-PCR analysis of *Pou5f1* and *Dppa3 (Stella)* expression in 13.5 dpc control (*Ctnnb1*$^{flox/flox,}$ gray) and *Sox2-CreERT2; Ctnnb1*$^{flox/flox}$ (dotted gray) ovaries. Student's *t* test, unpaired. Bars represent mean + SEM; *n* = 10 individual gonads. ***P* < 0.01; ****P* < 0.001.

(Fig. 6 *A* and *B*). Strikingly, whereas *Stra8* expression was lost in the majority of the germ cells in *Wt1-CreERT2;Ctnnb1*$^{flox/flox}$ gonads at 13.5 dpc (Fig. 1), *Stra8*-positive germ cells were readily detected in the *Sox2-CreERT2;Ctnnb1*$^{flox/flox}$ ovaries but not in controls at 12.5 dpc and were present in both genotypes at 13.5 dpc (Fig. 6*A*). qRT-PCR revealed a robust and precocious increase in *Stra8* expression in *Sox2-CreERT2;Ctnnb1*$^{flox/flox}$ germ cells at 12.5 dpc compared to their control germ cells, reaching the same levels of expression one day later in control and mutant germ cells (Fig. 6*B*), indicating that gonocytes have precociously differentiated as oocytes and initiated meiosis.

In contrast to the loss of *Bmp2* expression in *Wt1-CreERT2;Ctnnb1*$^{flox/flox}$ gonads, *Bmp2* expression was not affected in *Sox2-CreERT2;Ctnnb1*$^{flox/flox}$ ovaries, confirming that the somatic environment was not modified by *Ctnnb1* deletion in germ cells (Fig. 6 *A* and *B*). Moreover, *Bmp2* was already expressed at 12.5 dpc in both control and *Sox2-CreERT2;Ctnnb1*$^{flox/flox}$ ovaries, indicating that gonocytes required cell-intrinsic WNT/β-catenin activity to regulate the timing of meiosis entry, in addition to somatic signals stimulating the oogenic fate.

β-Catenin Stabilization Extends the Pluripotency Phase in Germ Cells. To determine whether stabilizing β-catenin impairs gonocyte differentiation, we used a loss-of-function model of GSK3β, a key kinase of the degradation complex of β-catenin (53). Immunostaining experiments revealed that GSK3β was present in the cytoplasm of both germ cells and somatic cells in the ovary at 13.5 dpc (Fig. 7*A* and *SI Appendix*, Fig. S7), suggesting that GSK3β-mediated regulation of β-catenin levels was active in both cell types. Moreover, its mRNA levels, measured in germ cells purified by FACS, increased as they differentiated (Fig. 7*C*). We next confirmed that the genetic ablation of *Gsk3β* stabilized WNT/β-catenin activity as evidenced by strong expression of LEF1 and an up-regulation of *Axin2* expression in *Gsk3β*$^{-/-}$ ovaries (Fig. 7 *A* and *E*). Importantly, GSK3β protein was absent in *Gsk3β*$^{-/-}$ ovaries, in contrast to control littermates. We conclude that genetic deletion of *Gsk3β* ectopically maintained WNT/β-catenin signaling activity in the developing ovaries.

Next, we addressed the proliferative behavior of gonocytes in *Gsk3β*$^{-/-}$ ovaries, by injection of Bromo-deoxyUridine (BrdU) over a 3 h timeframe and quantification of the number of BrdU-positive germ cells versus total germ cells at 13.5 dpc (Fig. 7*B*). This number was significantly increased in the *Gsk3β*$^{-/-}$ ovaries compared to the controls (Fig. 7*D*). We next investigated the differentiating state of gonocytes in absence of *Gsk3β*. The expression levels of the pluripotency-associated markers *Pou5f1*, *Sox2*, and *Nanog* mRNA were significantly increased in the mutant ovaries compared to the controls at 13.5 dpc (Fig. 7*E*). This was accompanied by an increase in the percentage of POU5F1- and SSEA1-positive germ cells and a decrease in the percentage of DAZL- and DDX4-positive germ cells in the absence of *Gsk3β* (Fig. 7*F* and *SI Appendix*, Fig. S7). This indicates that β-catenin ectopic stabilization led to the maintenance of pluripotency in gonocytes, which prevented them from differentiating as they normally would in control ovaries. Note that the lethality of the *Gsk3β*$^{-/-}$ embryos at 13.5 dpc prevented us analyzing when and whether meiosis was initiated in the absence of *Gsk3β*. Together, these results indicate that inhibiting WNT/β-catenin activity is required for gonocyte differentiation.

WNT/β-Catenin Signaling is Extinguished while Gonocytes Differentiate. Given the crucial role of β-catenin signaling in regulating the timing of gonocyte differentiation, we decided to investigate the temporal window of β-catenin activity in the embryonic ovary. To this aim, we performed a time-course analysis of the expression of known markers of canonical WNT/β-catenin signaling (i.e., β-catenin, POU5F1, *Lef1*/LEF1 and *Axin2*) (54–56) by immunostaining and RNAscope in situ hybridization in mouse ovaries at 11.5 dpc when primordial germ cells have just colonized the gonad in mice, 12.5 dpc when somatic cells are sexually differentiated, 13.5 dpc when germ cells initiate meiosis, and 14.5 dpc when they

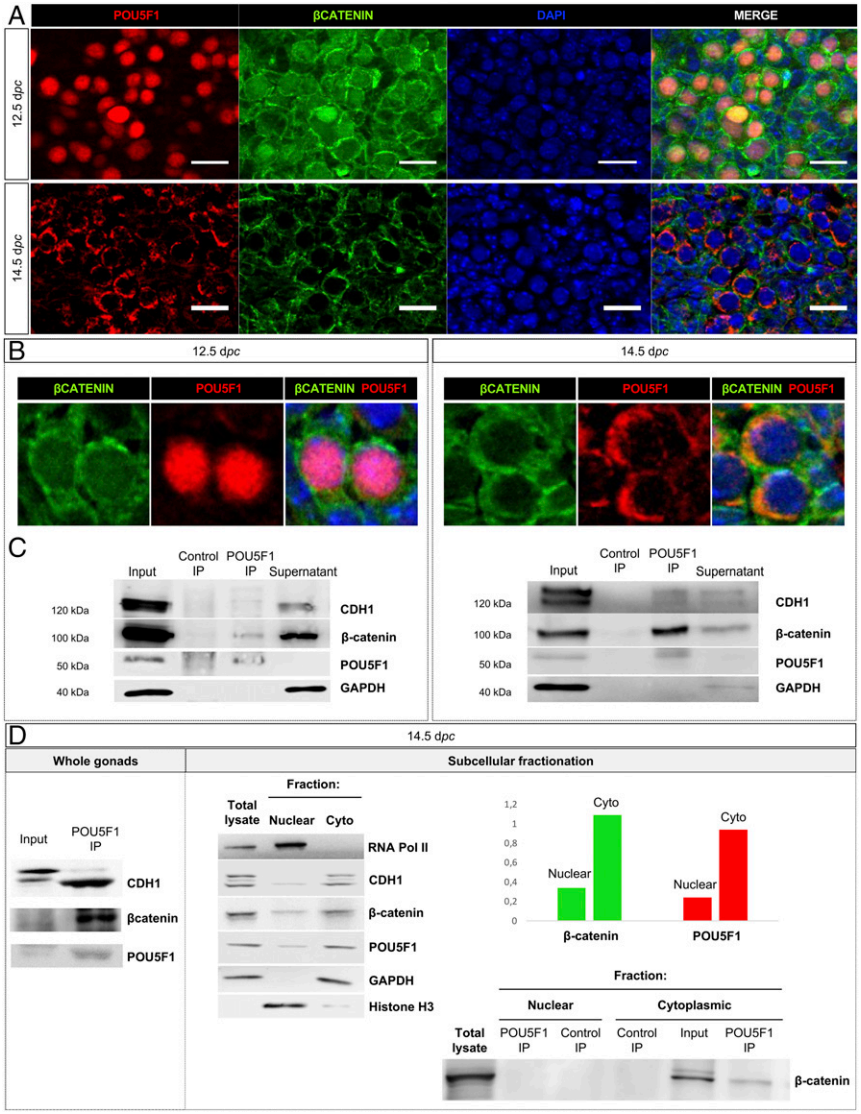

Fig. 5. POU5F1 and β-catenin physically interact during gonocyte differentiation. (*A*) Immunodetection of POU5F1 (red) and β-catenin (green) in 12.5 and 14.5 dpc wild-type ovaries. DAPI (blue): nuclei. (*B*) High magnification of immunodetection of POU5F1 (red) and β-catenin (green) in 12.5 and 14.5 dpc wild-type ovaries. DAPI (blue): nuclei. (*C*) Immunodetection by Western blot of β-catenin, POU5F1, CDH1, and GAPDH directly in protein lysate ("input") or in pellets after immunoprecipitation with control IgG ("control IP") or with POU5F1-raised specific antibody ("POU5F1 IP") or in immunoprecipitation supernatant ("supernatant") at 12.5 (*Left*) and 14.5 (*Right*) dpc ovaries. (*D*) Immunodetection by Western blot of β-catenin, POU5F1, RNA Polymerase II and Histone H3 (as controls for nuclear fraction), CDH1, and GAPDH (as controls for cytoplasmic/membranous fraction) either on whole 14.5 dpc ovaries (*Left*) or after subcellular fractionation (*Middle* and *Right*) in total cell lysate, nuclear and cytoplasmic fractions, before (*Middle*) and after immunoprecipitation with control IgG ("control IP") or with specific anti-POU5F1 antibody ("POU5F1 IP") (*Right*). Histograms: quantification of the expression of β-catenin (green) and POU5F1 (red) after Western blot in nuclear and cytoplasmic fractions (nuclear or cytoplasmic expression normalized with the total expression for each protein).

are progressing to meiosis. Immuno-localization experiments on wild-type ovaries revealed that LEF1 was strongly expressed in the nucleus of germ cells at 11.5, 12.5, and 13.5 dpc and was then down-regulated at 14.5 dpc (*SI Appendix*, Fig. S8 *A* and *C*). *Lef1* mRNA levels were significantly down-regulated in purified germ cells as they progressed toward differentiation (*SI Appendix*, Fig. S8*D*). In addition, β-catenin was strongly expressed in the nucleus, cytoplasm, and membrane of both somatic cells and germ cells at 11.5 and 12.5 dpc (*SI Appendix*, Fig. S8*B*). The expression then slightly decreased at 13.5 dpc (as quantified in *SI Appendix*, Fig. S8*C*), becoming located in the cytoplasm and at cell membrane at 14.5 dpc. These results were corroborated with *Axin2* RNAscope in situ hybridization analysis showing that, whereas almost 100% of the germ cells expressed *Axin2* at 12.5 dpc, *Axin2* expression was severely reduced or even absent in germ cells at 14.5 dpc (*SI Appendix*, Fig. S8*E*). Together, our data show that WNT/β-catenin pathway, initially active in gonocytes, was progressively repressed while they differentiated.

ZNRF3, an Inhibitor of WNT/β-Catenin Activity, Positively Regulates Germ Cell Differentiation. To investigate the mechanism by which WNT/β-catenin pathway was progressively inhibited during germ cell differentiation, we examined the expression of ZNRF3, a repressor of WNT/β-catenin signaling that is expressed in ovaries (57). We found that about 25% of germ cells expressed *Znrf3* mRNA at 12.5 dpc, whereas this number increased to 75% at 14.5 dpc (Fig. 8 *A* and *B*). Remarkably, this increase was correlated with the down-regulation of WNT/β-catenin signaling between 12.5 and 14.5 dpc (*SI Appendix*, Fig. S8), suggesting that *Znrf3* negatively regulates WNT/β-catenin activity in the differentiating germ cells.

To test the claim that ZNRF3 promotes the inactivation of WNT/β-catenin signaling in gonocytes, we analyzed the differentiation state of germ cells in the absence of *Znrf3*. As *Znrf3* is not only expressed in germ cells but also in ovarian somatic cells (Fig. 8*A*), we first confirmed that the supporting cells of the $Znrf3^{-/-}$ ovary differentiated as ovarian granulosa cells, expressing FOXL2, and not as testicular cells expressing SOX9 (Fig. 8*C*). In the $Znrf3^{-/-}$ ovaries, the majority of the germ cells maintained POU5F1 expression and did not enter meiosis as evidenced by the reduced SCP3 expression (Fig. 8*D*), demonstrating that ZNRF3 is required for the repression of WNT/β-catenin signaling in gonocytes, thus allowing them to exit the pluripotent state and differentiate.

WNT/β-Catenin Signaling Activity Controls the Genetic Program of Gonocyte Differentiation and Entry into Meiosis. Finally, to complete the analysis of the gonocyte phenotype of the four mutant

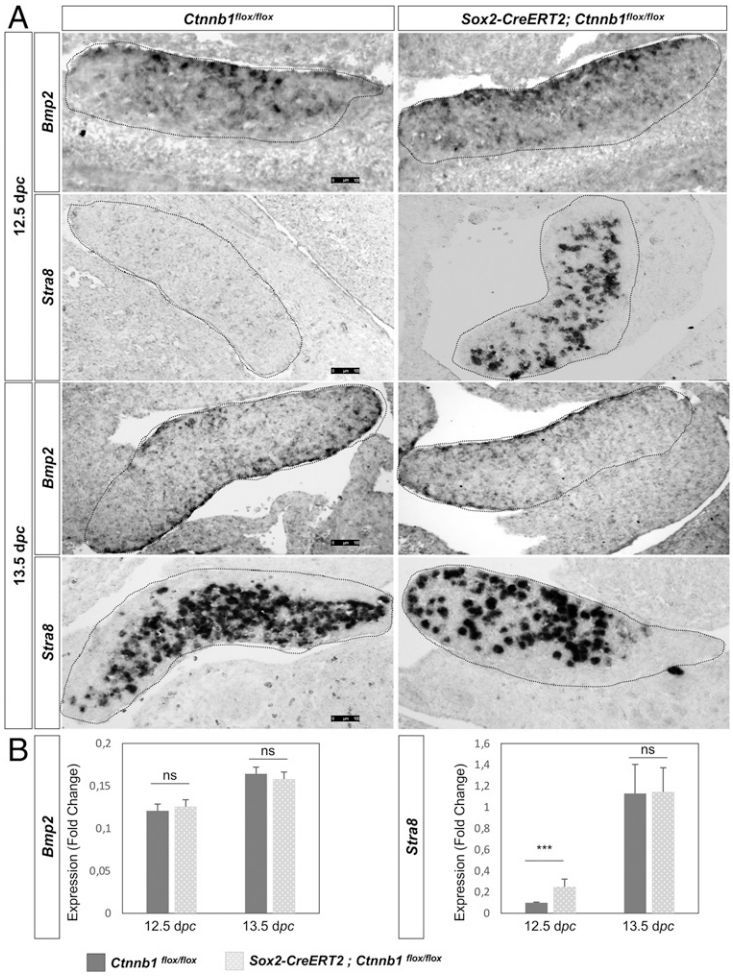

Fig. 6. Genetic ablation of *Ctnnb1* in gonocytes triggers precocious meiosis initiation. (*A*) In situ hybridization using *Bmp2* and *Stra8* riboprobes at 12.5 and 13.5 dpc in control (*Ctnnb1*$^{flox/flox}$, *left*) and *Sox2-CreERT2; Ctnnb1*$^{flox/flox}$ (mutant, *Right*) ovaries (dotted circles). (Scale bars: 50 μm.) (*B*) qRT-PCR analysis of levels of *Bmp2* and *Stra8* expression in 12.5 and 13.5 dpc control (*Ctnnb1*$^{flox/flox}$, dark gray) and *Sox2-CreERT2; Ctnnb1*$^{flox/flox}$ (dotted gray) ovaries. Student's *t* test, unpaired. Bars represent mean + SEM; $n = 6$ pairs of ovaries for each genotype and each age. ***$P < 0.001$; ns not significant.

mouse lines, we designed an qRT-PCR assay in which we compared the fold changes of the relative expression of 19 key genes involved in germ cell fate, as described in refs. 42, 58, and 59 (*SI Appendix*, Fig. S9*A*). At 12.5 dpc, the *Sox2-CreERT2;Ctnnb1*$^{flox/flox}$ gonocytes were clearly distinct in their expression profiles compared to the other mutant genotypes, as the cluster of genes involved in pluripotency such as *Dppa3*, *Nanog*, and *Pou5f1* was down-regulated, whereas the cluster of genes involved in meiosis such as *MeioC*, *Stra8*, and *Rec8* was up-regulated. These expression profiling data confirm that these gonocytes have precociously differentiated as oocytes and initiated meiosis. By contrast, in the *Wt1-CreERT2;Ctnnb1*$^{flox/flox}$ gonads, gonocytes maintained a pluripotency-associated program and were prevented from entering meiosis at 13.5 dpc as evidenced by the absence of up-regulation of the expression of meiotic genes. In addition, a proportion of these gonocytes adopted a male fate as indicated by *Nanos2* up-regulation (*SI Appendix*, Fig. S9*A*), further illustrating that WNT/β-catenin activity in somatic cells regulates the crosstalk between somatic cells and gonocytes and, indirectly, their sexual differentiation and entry into meiosis. In contrast, gonocytes in the *Znrf3*$^{-/-}$ and *Gsk3β*$^{-/-}$ ovaries exhibited a significant increase in the expression of the pluripotency genes (*Pou5f1*, *Nanog*, *Dppa3*) and a decrease in the expression of several meiotic genes such as *Scp3* or *Prdm9* compared to control ovaries (*SI Appendix*, Fig. S9*A*), confirming that ZNRF3 and GSK3β activities promote gonocyte exit from pluripotency. Nevertheless, in these mutants, gonocytes appeared to comprise a mixed population, with some gonocytes maintaining pluripotency and others initiating meiosis, indicating that ZNRF3- and GSK3β-regulated WNT/β-catenin activities regulate the fate of the whole gonad including somatic cells to synchronize gonocyte development. Together, these results provide an overall picture of gonocyte gene-expression changes in pathophysiological situations in which WNT/β-catenin activity is deregulated.

Discussion

In mice, once germ cells have colonized the gonad, they undergo profound changes in gene expression, DNA methylation, and behavior, thus acquiring the capacity to undertake sexual differentiation and becoming competent for gametogenesis, a process referred to as licensing (2). Eventually, germ cells initiate meiosis in XX gonads, whereas they stay quiescent in XY gonads. Whether these changes are cell-autonomous, programmed according to some intrinsic clock, or are induced in response to the new somatic environment, is still a matter of debate. On the one hand, XX germ cells enter meiosis in a wave that propagates from the anterior to posterior gonadal pole, suggesting that meiosis initiation depends on an intrinsic clock with the oldest germ cells first colonizing the anterior pole of the ovaries (60). On the other hand, germ cells are primed to enter meiosis when they are not in a testicular environment (3, 61, 62). Notably, germ cell licensing, which is required for meiotic onset (2), is regulated by diffusible signals synthesized by the somatic environment of the ovary (63), including ATRA (64), BMP2 (at least in vitro) (43), and by the RSPO1/WNT/β-catenin signaling pathway (31). We have previously shown that the genetic deletion of *Rspo1*, an agonist of WNT/β-catenin signaling produced by somatic cells, impairs germ cell proliferation, sexual differentiation, and subsequently meiosis

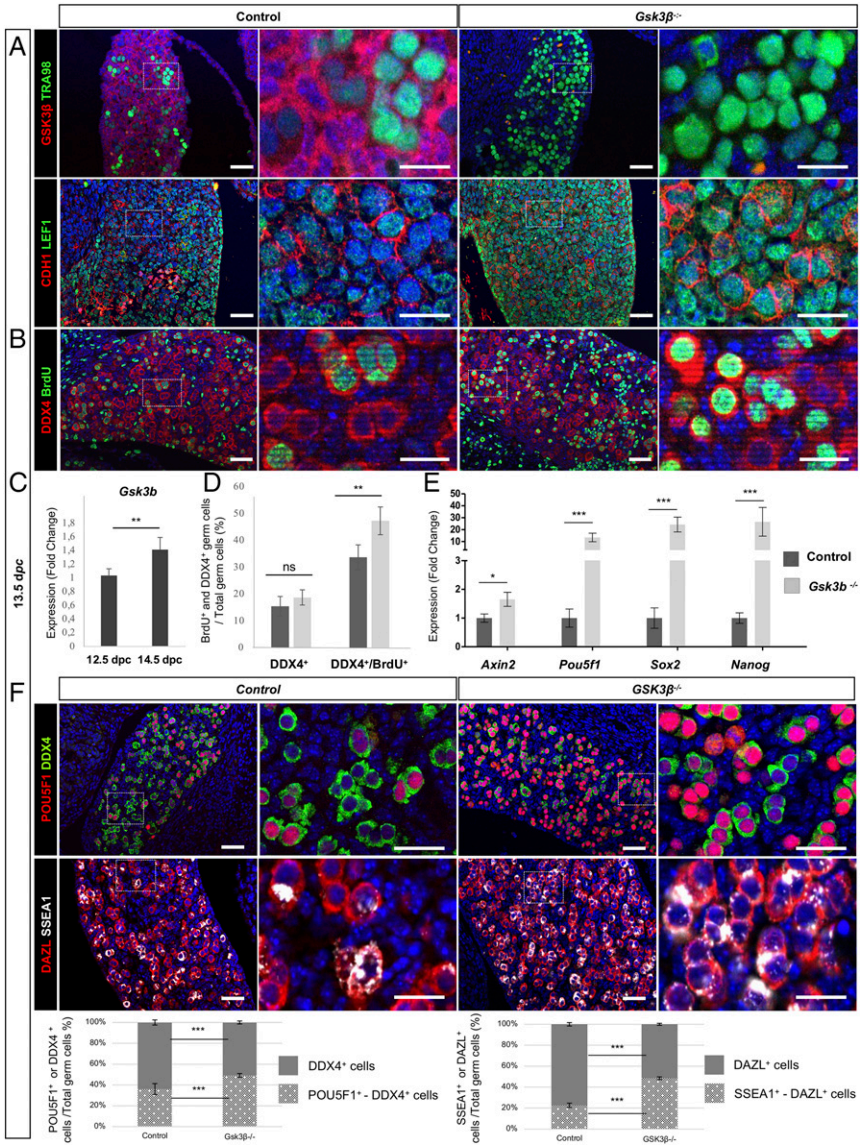

Fig. 7. β-catenin stabilization through GSK3β ablation leads to the maintenance of pluripotency in germ cells. (*A*) Immunodetection of GSK3β (red) and TRA98 (germ cells, green) and CDH1 (red) and LEF1 (green) in 13.5 dpc control and *Gsk3β*$^{-/-}$ ovaries. DAPI (blue): nuclei. (Scale bars: 50 or 20 μm.) (*B*) Immunodetection of DDX4 (germ cells, red) and BrdU (proliferating cells, green) in 13.5 dpc control and *Gsk3β*$^{-/-}$ ovaries. DAPI (blue): nuclei. (Scale bars: 50 or 20 μm.) (*C*) qRT-PCR analysis of *Gsk3b* expression in 12.5 and 14.5 dpc control FAC-sorted germ cells. Student's *t* test, unpaired. Bars represent mean + SEM; $n = 10$ individual ovaries. $^{**}P < 0.01$. (*D*) Histograms: quantification of DDX4-positive cells (germ cells, dark gray) and BrdU-DDX4 double positive cells (proliferating germ cells, dotted gray) (%) in control and *Gsk3β*$^{-/-}$ ovaries from 13.5 dpc embryos. Student's *t* test, unpaired. Bars represent mean + SEM. $^{*}P < 0.05$; $^{**}P < 0.01$. (*E*) qRT-PCR analysis of *Axin2*, *Pou5f1*, *Sox2*, and *Nanog* expression in 13.5 dpc control (dark gray) and *Gsk3β*$^{-/-}$ (dotted gray) ovaries. Student's *t* test, unpaired. Bars represent mean + SEM; $n = 10$ individual gonads. $^{*}P < 0.05$; $^{***}P < 0.001$. (*F*) Immunodetection of POU5F1 (red) and DDX4 (green) and DAZL (red) and SSEA1 (FUT4, white) in 13.5 dpc control and *Gsk3β*$^{-/-}$ ovaries. (Scale bars: 50 or 20 μm.) Histograms: quantification of DDX4-positive cells (pale gray) and POU5F1-DDX4 double positive cells (dotted gray) (%) and DAZL-positive cells (pale gray) and SSEA1-DAZL double positive cells (dotted gray) (%) in control and *Gsk3β*$^{-/-}$ ovaries from 13.5 dpc embryos after immunodetection. Student's *t* test, unpaired. Bars represent mean + SEM. $^{***}P < 0.001$.

initiation in the mouse ovaries (31). Hence, in the XX *Rspo1*$^{-/-}$ gonads, the majority of the gonocytes maintained POU5F1 expression and failed to express *Stra8*. Nevertheless, the germ-cell specific deletion of *Ctnnb1* has never been performed, preventing investigation of the cell-autonomous function of WNT/β-catenin signaling in female gonocytes.

To investigate the mechanism of action of WNT/β-catenin in oogenesis and discriminate its roles between different ovarian cell types, we used distinct genetic models, either to deplete *Ctnnb1* from gonocytes (*Sox2-CreERT2;Ctnnb1*$^{flox/flox}$ mice) or from somatic progenitor cells (*Wt1-CreERT2;Ctnnb1*$^{flox/flox}$ mice). Here, we show that genetic deletion of *Ctnnb1* in gonocytes triggered a premature exit from the mitotic cell cycle and a precocious meiosis onset, in contrast to genetic deletion of *Rspo1* (31) and to *Ctnnb1* deletion in WT1-positive cells (reported here), whereas stabilization of *Ctnnb1* caused a delay in cell cycle progression, a phenotype also reported by others in a PGC-specific *Ctnnb1* gain-of-function model (65). Moreover, β-catenin and POU5F1 expression, localization, and activity are closely aligned during germ cell differentiation, and they associate in the nucleus and maintain pluripotency in gonocytes. Whereas WNT is required to maintain the pluripotency of female gonocytes, it is critical that the gonocytes exit this state to enter meiosis. Our data show that down-regulation of WNT/β-catenin signaling is correlated with *Znrf3* up-regulation and with GSK3β up-regulation, both involved in β-catenin degradation (35, 36). The inhibition of WNT/β-catenin activation and the reduction of β-catenin accumulation in the nucleus is concomitant with POU5F1 and β-catenin exit from the nucleus, thus decreasing the expression of POU5F1 target genes and allowing germ cell differentiation and meiosis to occur (*SI Appendix*, Fig. S9). In conclusion, we propose that a fine-tuned arrest of WNT/β-catenin signaling intrinsically promotes germ cell differentiation and meiosis initiation. So far, how ZNRF3 and *Gsk3β* become up-regulated in germ cells remains to be investigated. In addition, it remains to be determined how POU5F1 and β-catenin precisely interact at a molecular level. Moreover, further evidence is required to identify by which mechanism these two factors are kept away from their target loci and translocated from the nucleus to the cytoplasm of the germ cells. Do POU5F1 and β-catenin have another function once they translocate to the cytoplasm is another remaining question. A model of free, nondirectional nuclear-cytoplasm diffusion of β-catenin has been proposed, its distribution being solely regulated by its retention in the nucleus though interaction with other cellular components, its

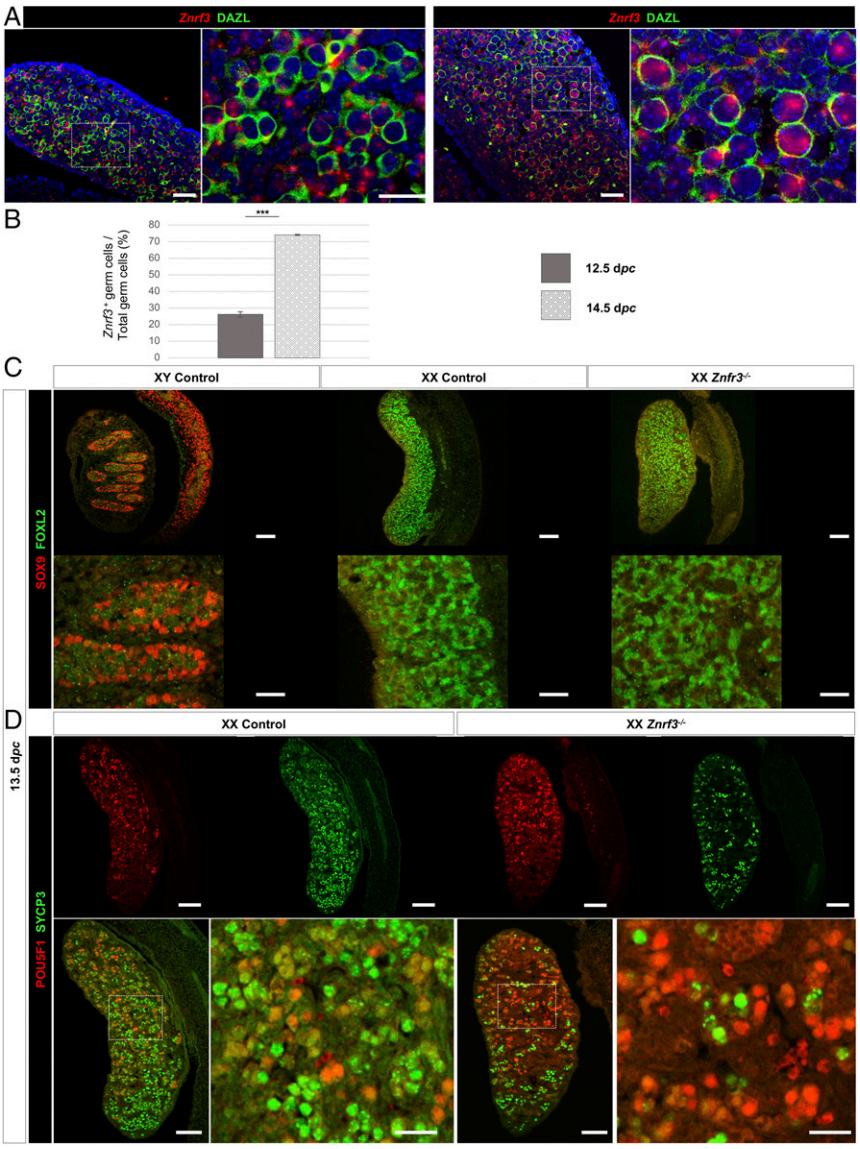

Fig. 8. ZNRF3, an inhibitor of WNT/β-catenin activity, positively regulates gonocyte differentiation. (*A*) RNAscope in situ hybridization using *Znrf3* riboprobe (red) and immunodetection of DAZL (green) in 12.5 and 14.5 dpc wild-type ovaries. (*B*) Histograms: quantification of the percentage of *Znrf3*-DAZL double positive cells versus DAZL-positive cells in 12.5 (gray) and 14.5 (dotted gray) dpc ovaries. Student's *t* test, unpaired. Bars represent mean + SEM. ***$P < 0.001$. (*C*) Immunodetection of SOX9 (red) and FOXL2 (green) in 13.5 dpc XY, XX control, and *Znrf3*$^{-/-}$ gonads. DAPI (blue): nuclei. (Scale bars: 50 or 25 μm.) (*D*) Immunodetection of POU5F1 (red) and SCP3 (green) in 13.5 dpc XY, XX control, and *Znrf3*$^{-/-}$ gonads. DAPI (blue): nuclei. (Scale bars: 50 or 25 μm.)

sequestration at the cell membrane with adhesion molecules such as CDH1, and its degradation in the cytoplasm by the proteasome (66). It has been described that POU5F1 is down-regulated along the length of the gonad during over the 13.5 and 14.5 dpc stages, a down-regulation coincident with the onset of meiosis (11, 67). After 14.5 dpc, rare female germ cells expressing POU5F1 remain and POU5F1 expression is completely extinguished by 16.5 dpc in the ovary. Together, these observations and our results suggest that POU5F1 and β-catenin are translocated in the cytoplasm of the germ cells, transiently associate with CDH1 and both factors are then rapidly degraded. Further studies should help us learn more about β-catenin and POU5F1 stability and localization and about their interacting partners in germ cells in vivo.

It is noteworthy that WNT/β-catenin signaling regulates the expression of *Bmp2* in ovarian somatic cells, a factor which is involved, once secreted, in instructing meiosis initiation in surrounding germ cells. These results provide an explanation for the inability of gonocytes to enter meiosis in *Rspo1* mutants (31). Together, this shows that meiosis entry in a timely manner requires the activity of WNT/β-catenin signaling in gonocytes to maintain pluripotency. Once WNT/β-catenin is down-regulated in gonocytes, signaling factors produced upon somatic WNT/β-catenin activity, such as *Bmp2*, enable the progression of gonocytes into meiosis.

Interestingly, we have previously shown that genetic ablation of *Rspo1* accelerates the differentiation of pregranulosa cells into mature granulosa cells that eventually transdifferentiate into Sertoli-like cells (28). In light of the results reported in the present study, we propose that the WNT/β-catenin pathway is a central gatekeeper, determining the proper timing of differentiation in somatic cells, enabling gonocytes to become oogonia and coordinating the development of the different cell types of the fetal ovary.

Well-timed progression of gonocytes toward gametogenesis depends on a complex epigenetic reprogramming process mediated by DNA demethylation, TET1 methylcytosine dioxygenase enzyme, and Polycomb Repressive Complex 1 (PRC1) (10), a large multiprotein complex acting in the female germline by silencing differentiation-inducing genes and defining appropriate chromatin states (9, 68). Impairing PRC1 function down-regulates the expression of POU5F1 and other pluripotency genes and abnormally activates *Stra8* transcription and the early meiotic program in gonocytes, thus promoting a premature transition from proliferation into meiosis (9). In addition, the transcription factor ZGLP1, a downstream effector of BMP2 signaling, positively

regulates the oogenic program by activating PRC-repressed genes using a molecular mechanism of action that is not yet clarified (13). Impairing PRC1 function (9) and deleting *Ctnnb1* in gonocytes (the present study) promote similar phenotypes, and we show here that β-catenin modulates chromatin accessibility in gonocytes. The role of β-catenin in chromatin remodeling has been previously shown in several somatic cell types, such as cardiomyocytes of the adult mammalian heart (69). Understanding the functional interactions between ZGPL1, PRC1, and β-catenin at the chromatin level will provide an integrated model for female gonocyte differentiation.

Primordial germ cells and pluripotent stem cells share common features such as alkaline phosphatase activity, expression of pluripotency factors, such as POU5F1, NANOG, and SOX2, and the capacity to be reprogrammed in vitro. In mouse ESCs (mESCs), WNT/β-catenin signaling regulates the maintenance and exit from the pluripotency state with various effects mostly depending on the culture conditions (70). In *Ctnnb1*-deficient mESCs, stemness is impaired, while activation of the WNT/β-catenin signaling by LiCl prolongs the expression of pluripotency genes, such as *Pou5f1*, *Nanog*, *Dppa4-5*, and delays the differentiation into embryoid bodies (71). Moreover, in mESCs grown in WNT3A-conditioned medium, β-catenin and POU5F1 physically interact, enhancing POU5F1 activity and eventually inhibiting neural differentiation and prolonging retention of pluripotency (72). Notably, POU5F1 and β-catenin collaborate to control cofactor exchange and chromatin accessibility on differentiation-related loci, thus integrating genomic responses to external cues such as WNT signals and directing lineage specification (73). Our results demonstrate that a similar collaboration between POU5F1 and β-catenin also exists in vivo during germ cell differentiation, thus providing a molecular explanation for the transition from undifferentiated germ cells to oogonia that eventually will be able to sustain gametogenesis.

Finally, human germ cell tumors, which are predominantly diagnosed in young patients, originate from germ cells that have retained or reactivated their embryonic pluripotency and self-renewal properties (74). Germ cell tumors express pluripotency markers such as POU5F1 or NANOG (75) and are often found to express β-catenin, which correlates with the degree of differentiation of the tumor (76). Given that WNT/β-catenin signaling regulates the timing of exit from the pluripotency-associated state in germ cells, it is also likely involved in the maintenance of this state in germ cell tumors. Our present study will not only propel future attempts to solve the complex puzzle of gametogenesis mechanisms but might also help clarify the etiology of cases of infertility and germ cell tumors.

Materials and Methods

Mouse Strains and Genotyping. The experiments described herein were carried out in compliance with the relevant institutional and French animal welfare laws, guidelines, and policies. All the experiments were approved by the French ethics committee (Comité Institutionnel d'Ethique Pour l'Animal de Laboratoire; number NCE-297). All mice were kept on a mix background 129/C57BL/6J. Mouse lines were obtained from the Jackson Laboratory. The *Wt1-CreERT2*, *Sox2*$^{tm1(cre/ERT)/Hoch}$ (or *Sox2-CreERT2*), *Ctnnb1*$^{tm2/Kem}$ (or *Ctnnb1*^{flox}), *Znrf3*^{flox}, *Gt(ROSA)26Sor*$^{tm4(ACTB-tdTomato,-EGFP)Luo}$, *GSK3β*, and *Axin2-CreERT2* mice were described previously and genotyped as reported (37, 39, 40, 44, 77–79). *Sox2-CreERT2*/+ mice are viable and normally fertile (40). Genotyping was performed using DNA extracted from tail tips or ear biopsies of mice.

To activate the CRE^{ERT2} recombinase in embryos, TAM (cat T5648, Sigma-Aldrich) was directly diluted in corn oil to a concentration of 40 mg/mL, and two tamoxifen (TAM) treatments (200 mg/kg body weight) were administrated to pregnant females by oral gavage at 9.5 and 10.5 dpc. This resulted in embryos in which *Ctnnb1* was deleted upon TAM induction when they were carrying the *Cre*^{ERT2} transgene as well as their control littermates. For proliferation assays, 5-Bromo-2′-deoxy-Uridine (BrdU) (cat B5002, Sigma-Aldrich) was diluted to a concentration of 10 mg/mL in sterile H_2O, was administrated to the pregnant females at a final concentration of 10 μg/mL by intraperitoneal injection, and pregnant females and their embryos were euthanized after 3 h.

qRT-PCR. Individual gonads without mesonephroi were dissected in phosphate buffered saline (PBS) from 11.5, 12.5, 13.5, and 14.5 dpc embryos. RNA was extracted using the RNeasy Qiagen kit and reverse transcribed using the RNA qRT-PCR kit (Stratagene). Primers and probes were designed by the Roche Assay Design Center (https://www.rocheappliedscience.com/sis/rtpcr/upl/adc.jsp). All RT-PCR assays were carried out using the LC-Faststart DNA Master kit Roche according to the manufacturer's instructions. qRT-PCR was performed on cDNA from one pair of gonads (n = 6 pairs of gonads per genotype and per age) and compared to a standard curve. qRT-PCR were repeated at least twice. Relative expression levels of each sample were quantified in the same run and normalized by measuring the amount of *Sdha* cDNA (which represents the total gonadal cells) with the 2-ΔΔCt calculation method.

Statistical Analysis. For each genotype, the mean of the absolute expression levels (i.e., normalized) was calculated, and graphs of qRT-PCR results show fold of change + SEM. All the data were analyzed by unpaired two-sided Student's t test using Microsoft Excel. Asterisks highlight the pertinent comparisons and indicate levels of significance: $*P < 0.05$, $**P < 0.01$, and $***P < 0.001$. Data are shown as mean + SEM.

Immunological Analyses. Samples were fixed with 4% (wt/vol) paraformaldehyde overnight and then processed either for paraffin embedding or directly for whole-mount immunostaining. Microtome sections of 5 μm thickness were processed for immunostaining. Immunofluorescence analyses were performed as described in ref. 31. The following dilutions of primary antibodies were used: CDH1 (cat 610182, BD Transduction Laboratories) 1:100, CTNNB1 (cat, C2206, Sigma-Aldrich) 1:100, active CTNNB1 (ABC) (cat 05-665, Millipore) 1:100, DAZL (cat GTX89448, Genetex) 1:200, DDX4/MVH (cat 13840, Abcam) 1:200, FOXL2 (cat 5096, Abcam) 1:300, GFP (cat TP401, Torrey Pines Biolabs) 1:750, GSK3β (cat 135653, Santa Cruz) 1:250, LEF1 (cat 137872, Abcam) 1:250, MKI67 (cat M3062, Spring Bioscience) 1:150, POU5F1 (cat 611202, BD Transduction Laboratories) 1:250, SCP3 (cat 15093, Abcam) 1:200, SOX2 (cat 97959, Abcam) 1:200, SOX9 (cat HPA001758, Sigma-Aldrich) 1:500, TRA98 (cat 82527, Abcam) 1:150, and FUT4 (SSEA1) (cat 21702, Santa Cruz) 1:200. Slides were counterstained with 4′,6-diamidino-2-phenylindole (DAPI) diluted in the mounting medium at 10 μg/mL (Vectashield, Vector Laboratories) to detect nuclei. Imaging was performed with a motorized Axio Imager Z1 microscope (Zeiss) coupled with an Axiocam Mrm camera (Zeiss), and images were processed with Axiovision LE and ImageJ. ImageJ software was used for quantification of proliferating germ cells versus total germ cells.

Cell imaging was performed with a Leica DM6000 TCS SP5 confocal microscope on an upright stand (Leica Microsystems, Mannheim, Germany), using objectives HC PL APO CORR 20X multi-immersion NA 0.7 and HCX APO L 63X oil 1.4 NA. The lasers used were argon laser (488 nm), HeNe laser (543 nm), and diodes laser 405 nm. The microscope was equipped with a galvanometric stage in order to do z-acquisitions, a resonant scanner and with an automated xy stage for mosaic acquisitions.

Data Availability. All study data are included in the article and/or *SI Appendix*.

ACKNOWLEDGMENTS. This work was supported by grants from the Agence Nationale de la Recherche (ANR-13-BSV2-0017-02 ARGONADS, ANR-20-CE14 ARDIGERM, and ANR-11-LABX-0028-01), Cancéropole PACA (Emergence), and Crédits Scientifiques Incitatifs Emergence from Nice Sophia Antipolis University. M.L.R. was supported by a fellowship from La Ligue Nationale contre le Cancer. A.S was supported by a grant from La Ligue Nationale Contre le Cancer (équipe labellisée Ligue Nationale Contre le Cancer). We acknowledge Dr. James Woodgett (Samuel Lunenfeld Research Institute, Toronto, Canada) for providing us the *Gsk3b* knockout mice. The microscopy was done at the Prism facility, "Plateforme PRISM," and the histological experiments were done at the "Experimental Histopathology Platform"—Institut de Biologie Valrose CNRS UMR 7277 Inserm U1091 UNS.

1. A. McLaren, Primordial germ cells in the mouse. *Dev. Biol.* **262**, 1–15 (2003).
2. M. E. Gill, Y. C. Hu, Y. Lin, D. C. Page, Licensing of gametogenesis, dependent on RNA binding protein DAZL, as a gateway to sexual differentiation of fetal germ cells. *Proc. Natl. Acad. Sci. U.S.A.* **108**, 7443–7448 (2011).
3. I. R. Adams, A. McLaren, Sexually dimorphic development of mouse primordial germ cells: Switching from oogenesis to spermatogenesis. *Development* **129**, 1155–1164 (2002).
4. M. H. Rosner *et al.*, A POU-domain transcription factor in early stem cells and germ cells of the mammalian embryo. *Nature* **345**, 686–692 (1990).

5. M. Saitou, M. Yamaji, Primordial germ cells in mice. *Cold Spring Harb. Perspect. Biol.* **4**, a008375 (2012).
6. A. McLaren, D. Southee, Entry of mouse embryonic germ cells into meiosis. *Dev. Biol.* **187**, 107–113 (1997).
7. Y. Ohkubo, Y. Shirayoshi, N. Nakatsuji, Autonomous regulation of proliferation and growth arrest in mouse primordial germ cells studied by mixed and clonal cultures. *Exp. Cell Res.* **222**, 291–297 (1996).
8. D. M. Maatouk *et al*., DNA methylation is a primary mechanism for silencing post-migratory primordial germ cell genes in both germ cell and somatic cell lineages. *Development* **133**, 3411–3418 (2006).
9. S. Yokobayashi *et al*., PRC1 coordinates timing of sexual differentiation of female primordial germ cells. *Nature* **495**, 236–240 (2013).
10. P. W. S. Hill *et al*., Epigenetic reprogramming enables the transition from primordial germ cell to gonocyte. *Nature* **555**, 392–396 (2018).
11. B. J. Lesch, G. A. Dokshin, R. A. Young, J. R. McCarrey, D. C. Page, A set of genes critical to development is epigenetically poised in mouse germ cells from fetal stages through completion of meiosis. *Proc. Natl. Acad. Sci. U.S.A.* **110**, 16061–16066 (2013).
12. M. Saitou, S. Kagiwada, K. Kurimoto, Epigenetic reprogramming in mouse pre-implantation development and primordial germ cells. *Development* **139**, 15–31 (2012).
13. S. I. Nagaoka *et al*., ZGLP1 is a determinant for the oogenic fate in mice. *Science* **367**, eaaw4115 (2020).
14. Q. Wu *et al*., Sexual fate change of XX germ cells caused by the deletion of SMAD4 and STRA8 independent of somatic sex reprogramming. *PLoS Biol.* **14**, e1002553 (2016).
15. A. E. Baltus *et al*., In germ cells of mouse embryonic ovaries, the decision to enter meiosis precedes premeiotic DNA replication. *Nat. Genet.* **38**, 1430–1434 (2006).
16. K. I. Ishiguro *et al*., MEIOSIN directs the switch from mitosis to meiosis in mammalian germ cells. *Dev. Cell* **52**, 429–445.e10 (2020).
17. J. Kehler *et al*., Oct4 is required for primordial germ cell survival. *EMBO Rep.* **5**, 1078–1083 (2004).
18. D. Okamura, Y. Tokitake, H. Niwa, Y. Matsui, Requirement of Oct3/4 function for germ cell specification. *Dev. Biol.* **317**, 576–584 (2008).
19. J. Bowles *et al*., Retinoid signaling determines germ cell fate in mice. *Science* **312**, 596–600 (2006).
20. J. Koubova *et al*., Retinoic acid regulates sex-specific timing of meiotic initiation in mice. *Proc. Natl. Acad. Sci. U.S.A.* **103**, 2474–2479 (2006).
21. A.-A. Chassot *et al*., Retinoic acid synthesis by ALDH1A proteins is dispensable for meiosis initiation in the mouse fetal ovary. *Sci. Adv.* **6**, eaaz1261 (2020).
22. N. Vernet *et al*., Meiosis occurs normally in the fetal ovary of mice lacking all retinoic acid receptors. *Sci. Adv.* **6**, eaaz1139 (2020).
23. A. A. Chassot *et al*., Constitutive WNT/CTNNB1 activation triggers spermatogonial stem cell proliferation and germ cell depletion. *Dev. Biol.* **426**, 17–27 (2017).
24. H. M. Takase, R. Nusse, Paracrine Wnt/β-catenin signaling mediates proliferation of undifferentiated spermatogonia in the adult mouse testis. *Proc. Natl. Acad. Sci. U.S.A.* **113**, E1489–E1497 (2016).
25. M. Tokue *et al*., SHISA6 confers resistance to differentiation-promoting Wnt/β-catenin signaling in mouse spermatogenic stem cells. *Stem Cell Rep.* **8**, 561–575 (2017).
26. S. Yoshida, Open niche regulation of mouse spermatogenic stem cells. *Dev. Growth Differ.* **60**, 542–552 (2018).
27. A. A. Chassot *et al*., Activation of beta-catenin signaling by Rspo1 controls differentiation of the mammalian ovary. *Hum. Mol. Genet.* **17**, 1264–1277 (2008).
28. D. M. Maatouk, L. Mork, A. A. Chassot, M. C. Chaboissier, B. Capel, Disruption of mitotic arrest precedes precocious differentiation and transdifferentiation of pregranulosa cells in the perinatal Wnt4 mutant ovary. *Dev. Biol.* **383**, 295–306 (2013).
29. S. Vainio, M. Heikkilä, A. Kispert, N. Chin, A. P. McMahon, Female development in mammals is regulated by Wnt-4 signalling. *Nature* **397**, 405–409 (1999).
30. B. Nicol, H. H. Yao, Gonadal identity in the absence of pro-testis factor SOX9 and pro-ovary factor beta-catenin in mice. *Biol. Reprod.* **93**, 35 (2015).
31. A. A. Chassot *et al*., RSPO1/β-catenin signaling pathway regulates oogonia differentiation and entry into meiosis in the mouse fetal ovary. *PLoS One* **6**, e25641 (2011).
32. F. Naillat *et al*., Wnt4/5a signalling coordinates cell adhesion and entry into meiosis during presumptive ovarian follicle development. *Hum. Mol. Genet.* **19**, 1539–1550 (2010).
33. H. Clevers, Wnt/beta-catenin signaling in development and disease. *Cell* **127**, 469–480 (2006).
34. D. Wu, W. Pan, GSK3: A multifaceted kinase in Wnt signaling. *Trends Biochem. Sci.* **35**, 161–168 (2010).
35. M. van Noort, J. Meeldijk, R. van der Zee, O. Destree, H. Clevers, Wnt signaling controls the phosphorylation status of β-catenin. *J. Biol. Chem.* **277**, 17901–17905 (2002).
36. M. Peifer, P. Polakis, Wnt signaling in oncogenesis and embryogenesis—A look outside the nucleus. *Science* **287**, 1606–1609 (2000).
37. B. K. Koo *et al*., Tumour suppressor RNF43 is a stem-cell E3 ligase that induces endocytosis of Wnt receptors. *Nature* **488**, 665–669 (2012).
38. H. X. Hao *et al*., ZNRF3 promotes Wnt receptor turnover in an R-spondin-sensitive manner. *Nature* **485**, 195–200 (2012).
39. B. Zhou *et al*., Epicardial progenitors contribute to the cardiomyocyte lineage in the developing heart. *Nature* **454**, 109–113 (2008).
40. K. Arnold *et al*., Sox2(+) adult stem and progenitor cells are important for tissue regeneration and survival of mice. *Cell Stem Cell* **9**, 317–329 (2011).
41. L. Mork *et al*., Temporal differences in granulosa cell specification in the ovary reflect distinct follicle fates in mice. *Biol. Reprod.* **86**, 37 (2012).
42. W. Niu, A. C. Spradling, Two distinct pathways of pregranulosa cell differentiation support follicle formation in the mouse ovary. *Proc. Natl. Acad. Sci. U.S.A.* **117**, 20015–20026 (2020).
43. H. Miyauchi *et al*., Bone morphogenetic protein and retinoic acid synergistically specify female germ-cell fate in mice. *EMBO J.* **36**, 3100–3119 (2017).
44. M. D. Muzumdar, B. Tasic, K. Miyamichi, L. Li, L. Luo, A global double-fluorescent Cre reporter mouse. *Genesis* **45**, 593–605 (2007).
45. Z. Liu, J. Wong, S. Y. Tsai, M. J. Tsai, B. W. O'Malley, Steroid receptor coactivator-1 (SRC-1) enhances ligand-dependent and receptor-dependent cell-free transcription of chromatin. *Proc. Natl. Acad. Sci. U.S.A.* **96**, 9485–9490 (1999).
46. V. Perissi *et al*., TBL1 and TBLR1 phosphorylation on regulated gene promoters overcomes dual CtBP and NCoR/SMRT transcriptional repression checkpoints. *Mol. Cell* **29**, 755–766 (2008).
47. R. R. Pandey *et al*., Tudor domain containing 12 (TDRD12) is essential for secondary PIWI interacting RNA biogenesis in mice. *Proc. Natl. Acad. Sci. U.S.A.* **110**, 16492–16497 (2013).
48. A. Loda, E. Heard, Xist RNA in action: Past, present, and future. *PLoS Genet.* **15**, e1008333 (2019).
49. M. Mark *et al*., Partially redundant functions of SRC-1 and TIF2 in postnatal survival and male reproduction. *Proc. Natl. Acad. Sci. U.S.A.* **101**, 4453–4458 (2004).
50. Y. Babaie *et al*., Analysis of Oct4-dependent transcriptional networks regulating self-renewal and pluripotency in human embryonic stem cells. *Stem Cells* **25**, 500–510 (2007).
51. D. N. Levasseur, J. Wang, M. O. Dorschner, J. A. Stamatoyannopoulos, S. H. Orkin, Oct4 dependence of chromatin structure within the extended Nanog locus in ES cells. *Genes Dev.* **22**, 575–580 (2008).
52. J. Bowles, R. P. Teasdale, K. James, P. Koopman, Dppa3 is a marker of pluripotency and has a human homologue that is expressed in germ cell tumours. *Cytogenet. Genome Res.* **101**, 261–265 (2003).
53. L. Kockeritz, B. Doble, S. Patel, J. R. Woodgett, Glycogen synthase kinase-3—an overview of an over-achieving protein kinase. *Curr. Drug Targets* **7**, 1377–1388 (2006).
54. M. F. Cole, S. E. Johnstone, J. J. Newman, M. H. Kagey, R. A. Young, Tcf3 is an integral component of the core regulatory circuitry of embryonic stem cells. *Genes Dev.* **22**, 746–755 (2008).
55. M. Filali, N. Cheng, D. Abbott, V. Leontiev, J. F. Engelhardt, Wnt-3A/β-catenin signaling induces transcription from the *LEF-1* promoter. *J. Biol. Chem.* **277**, 33398–33410 (2002).
56. B. Lustig *et al*., Negative feedback loop of Wnt signaling through upregulation of conductin/axin2 in colorectal and liver tumors. *Mol. Cell. Biol.* **22**, 1184–1193 (2002).
57. A. Harris *et al*., ZNRF3 functions in mammalian sex determination by inhibiting canonical WNT signaling. *Proc. Natl. Acad. Sci. U.S.A.* **115**, 5474–5479 (2018).
58. J.-J. Wang *et al*., Single-cell transcriptome landscape of ovarian cells during primordial follicle assembly in mice. *PLoS Biol.* **18**, e3001025 (2020).
59. C. Mayère *et al*., Single cell transcriptomics reveal temporal dynamics of critical regulators of germ cell fate during mouse sex determination. *FASEB J.* **35**, e21452 (2021).
60. D. B. Menke, J. Koubova, D. C. Page, Sexual differentiation of germ cells in XX mouse gonads occurs in an anterior-to-posterior wave. *Dev. Biol.* **262**, 303–312 (2003).
61. S. Dolci, M. De Felici, A study of meiosis in chimeric mouse fetal gonads. *Development* **109**, 37–40 (1990).
62. L. Zamboni, S. Upadhyay, Germ cell differentiation in mouse adrenal glands. *J. Exp. Zool.* **228**, 173–193 (1983).
63. Y. C. Hu *et al*., Licensing of primordial germ cells for gametogenesis depends on genital ridge signaling. *PLoS Genet.* **11**, e1005019 (2015).
64. H. Li, M. Clagett-Dame, A. Vitamin, Vitamin A deficiency blocks the initiation of meiosis of germ cells in the developing rat ovary in vivo. *Biol. Reprod.* **81**, 996–1001 (2009).
65. T. Kimura *et al*., The stabilization of beta-catenin leads to impaired primordial germ cell development via aberrant cell cycle progression. *Dev. Biol.* **300**, 545–553 (2006).
66. F. Fagotto, Looking beyond the Wnt pathway for the deep nature of β-catenin. *EMBO Rep.* **14**, 422–433 (2013).
67. M. Bullejos, P. Koopman, Germ cells enter meiosis in a rostro-caudal wave during development of the mouse ovary. *Mol. Reprod. Dev.* **68**, 422–428 (2004).
68. E. Posfai *et al*., Polycomb function during oogenesis is required for mouse embryonic development. *Genes Dev.* **26**, 920–932 (2012).
69. L. M. Iyer *et al*., A context-specific cardiac β-catenin and GATA4 interaction influences TCF7L2 occupancy and remodels chromatin driving disease progression in the adult heart. *Nucleic Acids Res.* **46**, 2850–2867 (2018).
70. J. Wray, C. Hartmann, WNTing embryonic stem cells. *Trends Cell Biol.* **22**, 159–168 (2012).
71. R. Anton, H. A. Kestler, M. Kühl, Beta-catenin signaling contributes to stemness and regulates early differentiation in murine embryonic stem cells. *FEBS Lett.* **581**, 5247–5254 (2007).
72. K. F. Kelly *et al*., β-catenin enhances Oct-4 activity and reinforces pluripotency through a TCF-independent mechanism. *Cell Stem Cell* **8**, 214–227 (2011).
73. Z. Simandi *et al*., OCT4 acts as an integrator of pluripotency and signal-induced differentiation. *Mol. Cell* **63**, 647–661 (2016).
74. Y. Atlasi, L. Looijenga, R. Fodde, Cancer stem cells, pluripotency, and cellular heterogeneity: A WNTer perspective. *Curr. Top. Dev. Biol.* **107**, 373–404 (2014).
75. J. W. Oosterhuis, L. H. J. Looijenga, Human germ cell tumours from a developmental perspective. *Nat. Rev. Cancer* **19**, 522–537 (2019).
76. F. Honecker *et al*., Involvement of E-cadherin and beta-catenin in germ cell tumours and in normal male fetal germ cell development. *J. Pathol.* **204**, 167–174 (2004).
77. R. van Amerongen, A. N. Bowman, R. Nusse, Developmental stage and time dictate the fate of Wnt/β-catenin-responsive stem cells in the mammary gland. *Cell Stem Cell* **11**, 387–400 (2012).
78. V. Brault *et al*., Inactivation of the beta-catenin gene by Wnt1-Cre-mediated deletion results in dramatic brain malformation and failure of craniofacial development. *Development* **128**, 1253–1264 (2001).
79. K. P. Hoeflich *et al*., Requirement for glycogen synthase kinase-3β in cell survival and NF-kappaB activation. *Nature* **406**, 86–90 (2000).